Desalination 468 (2019) 114073

Contents lists available at ScienceDirect

Desalination

journal homepage: www.elsevier.com/locate/desal

Lithium recovery from desalination brines using specific ion-exchange resins

Fátima Arroyo[a], José Morillo[a], José Usero[a], Daniel Rosado[b], Hicham El Bakouri[a,*]

[a] Department of Chemical and Environmental Engineering, University of Seville, Camino de los Descubrimientos, s/n. Isla de la Cartuja, 41092 Seville, Spain
[b] Department of Chemistry and Exact Sciences, Universidad Técnica Particular de Loja, 11 01 608 Loja, Ecuador

GRAPHICAL ABSTRACT

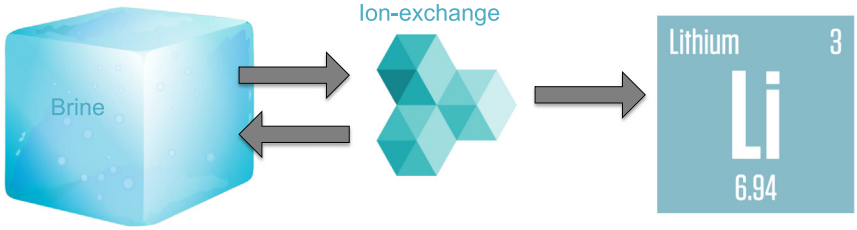

ARTICLE INFO

Keywords:
Lithium
Ion exchange
Brines
Recovery

ABSTRACT

This study evaluated the possibility of recovering lithium from brines by ion-exchange procedures. Three commercial ion-exchange resins were studied: K2629, TP207 and TP208.

Different tests have been carried out with artificial solutions and real brines. In addition, tests were carried out for Li elution, regeneration of the resins and reuse of the regenerated resins.

Sorption kinetics of lithium retention onto the three resins were studied and experimental data fit to the pseudo-second order kinetics model. Equilibrium sorption data were analysed by the Langmuir, Freundlich, Temkin and Dubinin-Radushkevic approaches. Langmuir isotherm model best described the process. The order of retention capacity of the amendments was TP207 > K2629 > TP208.

Recovering Li from brines was possible with ion exchange resins. In solutions containing only Li, the three resins studied had high retention yields (> 95%). The presence of other ions in solution negatively affects the behavior of the three resins studied.

Regarding desorption, yields obtained ranged 73.8% - 89.8%, reaching the highest (> 80%) using 4 M HCl as eluting solution. Regenerated resins showed similar yields to those obtained when the resin is used for the first time.

1. Introduction

The demand of Li has greatly increased in the last decades due to its applications in large-capacity rechargeable batteries, light aircraft alloys, cosmetics and pharmaceuticals applications. Furthermore, it is expected to continue growing in the future because of new applications, such as fuel for nuclear fusion [1].

Li is obtained mainly from two natural sources: the spodumene mineral, double silicate of Al and Li ($LiAlSi_2O_6$) associated with quartz, mica and feldspar, and the natural brines of the salt lakes and geysers, mainly in the form of double sulphates of Li and K ($KLiSO_4$) and other salts. Currently, brines provide the highest production at the lowest cost [2–4] by evaporation of water and the subsequent precipitation of some lithium compound.

* Corresponding author.
E-mail addresses: fatimarroyo@us.es (F. Arroyo), jmorillo@us.es (J. Morillo), usero@us.es (J. Usero), djrosado@utpl.edu.ec (D. Rosado), elbakouri@us.es (H. El Bakouri).

https://doi.org/10.1016/j.desal.2019.114073
Received 18 March 2019; Received in revised form 6 July 2019; Accepted 10 July 2019

If seawater is not considered, existing reserves of Li will be insufficient to cover the demand for this metal in the future. So, research is beginning to focus on extracting Li directly from seawater, where it is estimated at approximately $2.5{\cdot}10^{14}$ kg, or through brines generated in seawater desalination plants with reverse osmosis technology. The latter is interesting because of the large number of existing plants, their foreseeable growth and the fact that brine is more concentrated than seawater. This technology allows obtaining large quantities of Li and other valuable metals and, thus, helps the economic profitability of desalination brine management, which generates a significant environmental impact in the areas surrounding its discharge.

The incorporation of selective extraction technologies to the current desalination systems is challenging due to the low concentrations, the limited selectivity of the extractants and the complexity of the brine matrix. For this purpose, materials with high operating capacity and selectivity are required to avoid competition within alkaline and alkaline earth cations maintaining low operating costs. The main existing technologies for this purpose are: liquid-liquid extraction, ion exchange, leaching, precipitation, adsorption and electrochemical processes. At present, the processes for extracting Li from seawater and desalination brines are mainly based on membrane technologies, adsorption and ion exchange, although research on liquid-liquid extraction was carried out decades ago. Initially, the behavior of zirconium phosphate ($Zr_3(PO_4)_4$) was investigated and currently it is intended to extract the Li through various compounds of manganese oxide (MnO_2), a substance with a very high selectivity towards Li. The Lithium recovery from brines by membrane and/or electrochemical processes are relatively novel technologies becoming very important [5–11].

The most studied processes to recover Li from seawater require manufacturing a solid material morphologically modified with a Li solution that creates the active sites with greater selectivity for the Li. Research found has been divided according to the starting material with which the solid is manufactured: manganese oxides, aluminum compounds, exchange resins and other solids (Table 1).

- **Recovery through contact with modified resins**. Several patents have been found, dealing with the modification of anion exchange resins by contact with aluminum compounds. It involves the impregnation of an ion exchange resin with $AlCl_3$ and ammonia. After the impregnation, it is contacted with a Li halide (LiX) to form a Li aluminate, and subsequently heated until $LiX{\cdot}2\ Al(OH)_3$ is formed. Then, the LiX is removed from the solid and the modified resin allows the selective Li recovery in the presence of other elements such as Na, Ca, Mg, K and/or B. There are no substantial differences between the following patents, having even the same name [28–33].
- **Recovery through contact with commercial resins**. Few studies on the recovery of lithium by conventional ion exchange resins have been published [37].

Most of these processes have been designed for natural brines, and there are not many studies on metal recovery from industrial effluents. In this work, the recovery of lithium from synthetic solutions and from real brines the brine of a seawater desalination plant using reverse osmosis have been studied. With this aim, three low cost cationic ion exchange resins have been used. The influences of the contact time, the amount of lithium in the brines and the presence of an interfering element of great importance such as sodium have been studied. With these experimental data, It has been determined the load kinetics that is adjusted to the lithium retention with each type of resin, the equilibrium isotherms that best define the retention of lithium by the resins and a mathematical model has been developed that allows predict lithium retention in brines with different concentrations of Li and Na. The optimal conditions for elution of lithium and regeneration of resins have also been studied. Summing up, this work deepens in the knowledge about the retention of lithium from cationic and low cost resins from brines.

2. Materials and methods

2.1. Introduction to the experimental design

In this research, 5 different types of experiments were performed to analyze the capacity of three type of resins to capture Li in synthetic and real brines: kinetic studies, equilibrium studies, the elution and reutilization, effect of Na content studies and Li retention from real brines. Experiments, together with their operating conditions are detailed in Table 2.

In each test, 50 mL of synthetic brines (containing Li and/or Na) and resin were placed in 100 mL flasks and maintained in contact using a rotary shaker at 25 °C. Different synthetic brines/resin ratios, and different Li and/or Na contents were varied throughout the study. After the contact, resin and solution (raffinate) were separated using a membrane filter (0.45 μm) and the resins were washed twice with distilled water. Raffinates were analysed for Li content using Li retention efficiency (R) and capacity (Q) that were calculated according to Eq. (1) and Eq. (2). The loaded resin and eluting solution were contacted as described in sorption stage.

$$R\ (\%) = \frac{(C_0 - C_e)}{C_0}{\cdot}100 \tag{1}$$

$$Q\left(\frac{mg}{g}\right) = \frac{(C_0 - C_e){\cdot}V}{W} \tag{2}$$

where C_0 and C_e ($mg\ L^{-1}$) are the Li content in the solution initially and at equilibrium, respectively, V (L) is the volume of solution, and W (g) is the resin mass. The elements in the solution were analysed using an ICP-OES Agilent 5100.

Synthetic brines were used and prepared by dissolving weighed amount of LiCl and NaCl in ultrapure water, i.e. type 1 water (Merck Millipore, Germany). All other used chemicals were of analytical grade. A real sea-water reverse osmosis brine collected in a desalination plant located in Almería (Spain) was also used. Its composition is described in Table 3. The compositions of the different synthetic solutions are shown in Table 2.

Resins Lewatit K2629, TP 207 and TP 208 were obtained from Lanxess (Germany). Its characteristics are given in Table 4. Lewatit TP 207 and TP 208 are macroporous cation exchange weakly acidic resins with chelating groups for the selective removal of metal cations from solutions. Compared to Lewatit TP 207, TP 208 resin has a heterodispersed bead size, a modified polymer structure and a modified substitution grade of the imino-diacetate groups. Lewatit K2629 is a, macroporous, polymer-based strongly acidic resin.

Table 1
Technologies for the recovery of Li by adsorption in morphologically altered solid materials.

Lithium adsorption sorbents	References
Sorbents based on manganese oxide	([12]; [13,14]; [15]; [16]; [17]; [18]; [19]; [20])
Sorbents based on activated alumina and aluminum compounds	([21]; [22–24]; [25]; [26]; [27])
Modified resins	([28–32]; [33])
Sorbents based on zirconium phosphate from zirconium oxide	([34]; [35]; [36])
Commercial resins	[37]

Table 2
Experimental design.

	Resin mass (g)	Brine volume (ml)	Brine content (mg L^{-1})		Contact time (min)	Temperature (°C)	Elution		
			Li	Na			Eluting solution	Time (h)	Temperature (°C)
Kinetics studies	1	50	10	0	1–1440	25	–	–	–
Equilibrium studies	1	50	0.5–50	0	60	25	–	–	–
Elution and reutilization	1	50	10	0	60	25	HCl 3 M, 4 M	24	25
Effect of Na content			5–100	100–10,000	1440	25	–	–	–
Retention from real brines	1, 10, 20	50	0.6	15,300	1440	25	–	–	–

Table 3
Composition and properties of sea-water reverse osmosis brine collected in Almería (Spain) desalination plant.

Property	Value
Conductivity at 25 °C	73 mS cm^{-1}
pH	7.84
Alcalinity	445 mg $CaCO_3$ L^{-1}
Chloride	28.7 g L^{-1}
Sulfate	4.60 g SO_4 L^{-1}
Sodium	15.3 g L^{-1}
Lithium	0.60 mg L^{-1}

2.2. Kinetics studies

The kinetics tests were carried out by a batch technique according to the method described in Section 2.1. The obtained results were analysed using the pseudo-first and pseudo-second order kinetic equations. Pseudo-first-order kinetic model fits when sorption is driven by mass concentration gradient. The pseudo-second-order rate reaction is mostly concerned with the amount of metal on the adsorbent's surface at equilibrium [38]. The differential and integral forms of both models are shown in Eqs. (3) and (4).

$$\frac{dQ_t}{dt} = k_1 \bullet (Q_e - Q_t) \log(Q_e - Q_t) = \log Q_e - k_1 \bullet t \quad (3)$$

$$\frac{dQ_t}{dt} = k_2 \bullet (Q_e - Q_t)^2 \frac{t}{Q_t} = \frac{1}{k_2 \bullet Q_e^2} + \frac{1}{Q_e} \bullet t \quad (4)$$

where Q_t and Q_e are the amount of Li retained by each resin at any time t and at the equilibrium time respectively, calculated according to Eq. (2). k_1 (min^{-1}) and k_2 (g mg^{-1} min^{-1}) are the equilibrium rate constants of the pseudo-first-order and pseudo-second-order kinetics models respectively. If the retention rate is defined as $H = Q_t/t$ [39], when t approaches 0, H (meq g^{-1} h^{-1}) is the initial Li retention yield (Eq. (5)).

$$H = k_2 \bullet Q_e^2 \quad (5)$$

The integral forms of both models were used for the analysis of the kinetics and characteristic parameters determination [40]. Based on the results, the orders of reaction were determined. The linear plots of the models were made and k_1 and k_2 were obtained from the slopes. The values of k_1 and k_2 and the experimental and estimated values of Q_e are given with the determination coefficients of each model.

The suitability and precision of the kinetic models were tested by the chi-square (χ^2) (Eq. (6)).

$$\chi 2 = \frac{(Q_{eexp} - Q_{ecal})^2}{Q_{ecal}} \quad (6)$$

2.3. Equilibrium studies

Equilibrium experiments were conducted by the batch method. Kinetic studies indicated that 30 min of equilibration were sufficient to attain the equilibrium.

The retention yields (R) and the loading capacities (Q_e) at equilibrium were calculated according to Eq. (1) and Eq. (2), respectively. Results obtained were fitted to Langmuir, Freundlich, Temkin and Dubinin-Radushkevic models of equilibrium in ion-exchange. Isotherm models represent the equilibrium distribution of Li between the solid and liquid phases and illustrate the type of interaction between the Li ion and the resin in each case. The isotherm model can determine the maximum sorption capacity and several thermodynamic parameters that can be used for a better understanding of the sorption system.

Langmuir model describes quantitatively the formation of a monolayer adsorbate on the outer surface of the solid, and after that, no further retention takes place [41] and it describes the adsorption onto a surface containing a finite number of identical active sites. Langmuir represented the Eq. (7).

$$\frac{1}{Q_e} = \frac{1}{Q_M} + \frac{1}{K_L Q_M C_e} \quad (7)$$

where Q_e is the equilibrium amount of Li retained per unit resin mass in mg g^{-1}, Q_M (mg g^{-1}) is the maximum capacity and K_L (L mg^{-1}), named Langmuir isotherm constant, and is related to the energy of adsorption and to the affinity between Li and resin. The equilibrium dimensionless constant, R_L (Eq. (8)), is related to separation factor or equilibrium parameter [42] and indicates the retention nature (unfavorable if $R_L > 1$, linear if $R_L = 1$, or favorable if $0 < R_L < 1$).

$$R_L = \frac{1}{1 + (K_L + C_0)} \quad (8)$$

Freundlich model is commonly used to describe the adsorption onto heterogeneous surface [43]. These data often fit the empirical equation proposed by Freundlich (Eq. (9)):

$$Q_e = K_F C_e^{1/Fr} \quad (9)$$

where K_F is Freundlich isotherm constant (mg g^{-1}) is referred to the adsorption capacity. The exponent Fr is adsorption intensity, and 1/Fr is a function of the strength of adsorption in the adsorption process [44]. If Fr = 1 then the partition between solid and liquid phases is independent of the concentration. If value of 1/Fr < 1, it indicates a

Table 4
Properties of the resins Lewatit K2629, TP207 and TP 208 [data from Lanxess].

Resin	Matrix	Effective size	Active group	Ionic form	Bulk density (g L^{-1})	Capacity (eq/L)
Lewatit K2629	Crosslinked polyestirene	0.55 mm	Sulfonic acid	H^+	760	1.7
Lewatit TP 207			Imino-diacetatic acid	Na^+	720	2.2
Lewatit TP 208				Na^+	740	1.8

normal adsorption, and 1/Fr > 1 indicates cooperative adsorption [45]. If 1/Fr lies between one and ten, this indicates a favorable sorption process [46].

The Temkin Isotherm (Eq. (10)) contains a factor assessing adsorbent–adsorbate interactions. The model assumes that heat of adsorption of all molecules in the layer would decrease linearly with coverage [47]. It is characterized by a uniform distribution of binding energies that was carried out by plotting the quantity sorpted Qe against lnCe and the constants were determined from the slope and intercept [48].

$$Q_e = \frac{RT}{b_t} \ln(A_T C_e) \tag{10}$$

where A_T is the Temkin isotherm equilibrium binding constant ($L\,g^{-1}$), b_T is the Temkin constant, R is the universal gas constant ($8.314\,J\,mol^{-1}\,K^{-1}$) and T is defined equal to 298 K.

Dubinin–Radushkevich isotherm model (Eq. (11)) is generally applied to express the adsorption mechanism with a Gaussian energy distribution onto a heterogeneous surface [49,50].

$$Q_e = Q_s \exp(-K_{ad}\varepsilon^2) \tag{11}$$

where Qs is the theoretical isotherm saturation capacity ($mg\,g^{-1}$), K_{ad} is the Dubinin–Radushkevich isotherm constant ($mol^2\,kJ^{-2}$) and ε is the Dubinin–Radushkevich isotherm constant (Eq. (12)).

$$\varepsilon = RT \ln\left(1 + \frac{1}{C_e}\right) \tag{12}$$

2.4. Elution and reutilization studies

Loading efficiency was calculated by mass balance (eq. 13), and eluting efficiency was calculated according the following expression:

$$S_{Li} = \frac{C_s \cdot V_s}{(C_0 - C_e) \cdot V_R} \cdot 100 \tag{13}$$

where c_s is the Li content in the stripping solution after elution, Vs is the stripping solution volume (L), V_R is the working solution volume (L), c_o and c_e are the initial and equilibrium Li content of solutions (in loading step), in $mg\,L^{-1}$.

For reutilization experiments, resins were loaded and eluted under the experimental conditions showed in Table 2. After the elution, resins were carefully washed with water and each type of resin was divided in two identical parts, conditioned according to provider: one half to H form (using HCl) and the other to Na form (using NaCl). Once regenerated, the conditioned-resins were contacted with working solutions under the conditions described in Table 2. New sample of each resin were included in reutilization tests for comparative purposes.

2.5. Effect of Na content studies

The response surface methodology (RSM) technique based on a five-level, two-variable central composite rotatable design (CCRD) was employed. The Stat-Ease Design-Expert (version 9.0.6.2) software was used for experimental design and response surface design and analysis. The space of interest was defined by the following ranges: Na initial concentration: 100–15,000 ($mg\,L^{-1}$), and Li initial concentration: 0.5–100 ($mg\,L^{-1}$). The CCRD consisted of a total of 13 experiments for each resin (Fig. 1). Table SI-1 shows the design matrix. For statistical calculations experimental conditions are expressed in coded terms. The coded values of actual parameters could determinate by Eqs. (14) and (15).

$$Li\ coded\ content = \frac{Li\ actual\ content - 50}{30} \tag{14}$$

$$Na\ coded\ content = \frac{Na\ actual\ content - 5000}{3500} \tag{15}$$

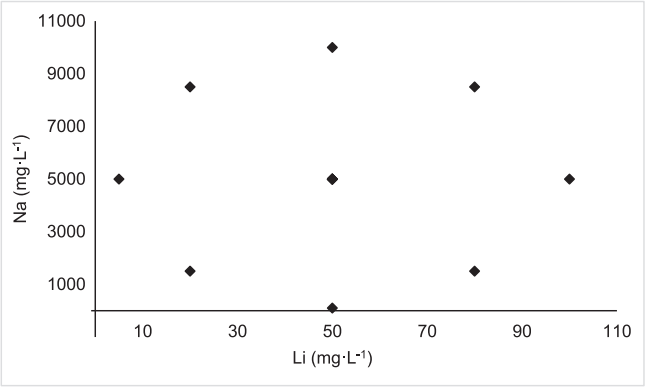

Fig. 1. Central composite rotatable design model.

where Li and Na coded contents are the "normalized" Li and Na contents in coded terms (adimensional), respectively. The actual Li and Na content of solutions are expressed in $mg\,L^{-1}$.

The experimental data were fitted by a polynomial equation (response surface) in order to determine the relationships between factors and the response variables. The predicted responses in the model are retention and capacity. First or third order polynomial equations are suggested too. Description is analogous. The quality of fit polynomial model was expressed by R^2 and the F-test model examined its statistical significance. The response surface mathematical models predicted the optimum Li retention conditions with each resins in solutions containing Li and Na.

3. Results and discussion

3.1. Kinetic studies. Effect of contact time

Experimental Li loading capacity of each resin was plotted as a function of contact time and it was observed that the loading capacity increased with time in all cases (Fig. 2). Two loading zones for the three resins are appreciated, a fast one (for the first 5 min), and then a very slow one (up to 20 min). Increasing time from 5 to 20 min, the retention increased only from 82.5% to 97.9% for TP 208, from 96% to 98% for TP207 and from 80% to 95% for K2629. The first loading zone could correspond to the stages of surface retention and diffusion within the pores of the resin, and would be very fast thanks to the small size of the Li. In the second charging zone, the controlling mechanism could be the diffusion of Li to the resins, due to the low concentration of Li in solution after the first 10 min of contact.

The coefficients of determination (R^2) obtained for the pseudo-first order model are lower than those obtained for the second order-models, indicating that the pseudo-second order kinetic equation described better the sorption process (Table 5). The high values of R^2 indicated that the models described successfully the Li retention onto the studied resins. Moreover, the experimental capacity values ($Q_{e\text{-}exp}$) are in agreement with the calculated values of sorption capacities from the second-order kinetic equation ($Q_{e\text{-}cal}$).

Values of χ^2 are low for the three resins: $7.8{\cdot}10^{-3}$ for K2629, $3.5{\cdot}10^{-3}$ for TP207 and $9.5{\cdot}10^{-4}$ for TP208. So the pseudo- second order kinetic model determined in this study can be considerate suitable and precise. In all cases equilibrium was achieved after 30 min, so the Li content at 30 min were used for k_1 and k_2 determination. As it is shown in Table 5, the fastest retention of Li is attributed to TP 208 (the highest rate constant), and the slowest for K2629. Compared to TP 207 and TP 208, K2629 showed lower initial rate (H) of ion exchange between resin and aqueous solution, which in agreement with k_2 values. The theoretical capacity at equilibrium sequence is TP 207 > K2629 > TP 208, but the values are quite similar, which is in agreement with the experimental values of capacity. The sequence of

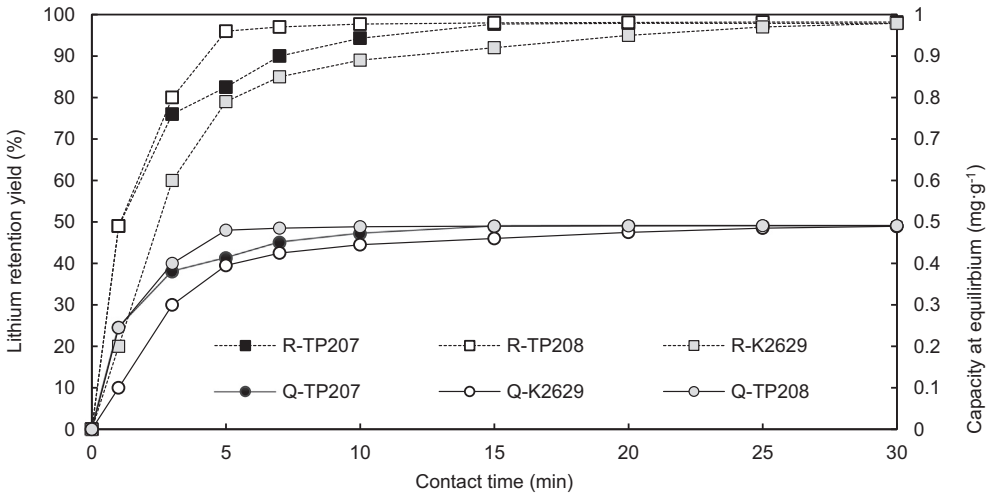

Fig. 2. Li retention yields and capacities at equilibrium during the first 30 min of contact for the resins TP 207, TP 208 and K2629.

theoretical capacities is quite similar to the order of capacities reported by the manufacturer.

Taking into account both criteria (R^2 and χ^2), results indicated that pseudo-second order was more suitable for the Li retention onto K2629, TP 207 and TP 208 resins. The better fit of the pseudo-second-order suggest that resins-Li main interaction is controlled by chemical sorption, and the retention rate depends more on the availability of the active sites than the concentration of Lithium in solution [51–53].

3.2. Equilibrium studies. Effect of initial Li concentration

The sorption data obtained were fitted to the different equilibrium models and the obtained linearized equations are summarized in Table SI-2.

If the three resins are compared, for low concentrations of Li ($< 5\ mg\ L^{-1}$), the distribution coefficient is much higher for the case of resin K2629 than in the case of resins TP 207 and TP 208, which show values similar to the distribution coefficient. When the concentration of Li is higher than $10\ mg\ L^{-1}$, the distribution coefficient is similar for the three resins. Therefore, if the solution has a low Li content, the K2629 will retain more Li than the TP 207 and TP 208 resins. From 10 mg Li L^{-1}, the behavior of the three resins will be similar.

Isotherm constants of Langmuir, Freundlich, Temkin and Dubinin-Radushkevic were obtained from the slopes and intercepts of linearized form of models. Constants and values of determination coefficients are shown in Table SI-2 and Table 6.

Although all models represent satisfactorily the adsorption process (showing high determination coefficients), it seems that the Langmuir and Freundlich isotherms ($R^2 > 0.946$) give a better fit than Temkin and Dubinin-Radushkevic models ($R^2 < 0.919$) for the three resins. So an analysis for both Langmuir and Freundlich models were performed for comparative reasons.

From the data calculated in Table SI-2, the Langmuir separation factor (R_L) is > 0 but < 1 in all experiments, indicating that equilibrium sorption is favorable for the 3 resins. For the 3 resins, R_L decreased when Li content increased, so the retention is favored at high Li contents. If the 3 resins are compared, TP 207 show a less R_L. The maximum monolayer coverage capacity (Q_M) from Langmuir model was achieved by TP 207 ($2.536\ mg\ g^{-1}$). The maximum K_L is also achieved with the resin TP 207. Therefore attending the Langmuir parameters, TP 207 is the resin showing more affinity with Li ions (the lowest R_L and the highest K_L and Q_M).

Regarding the Freundlich constants (Table SI- 2), as the 3 resins shown values of $1/Fr < 1$ (0.559–0.657), the sorption of Li^+ into 3 studied resins are favorable. The smaller value of (1/Fr) for resin K2629 indicated a stronger bond between Li and resin, but the values are quite similar.

Due to the determination factors of three resins values and the characteristics of resins (homogeneous sites), Langmuir model is preferred for describing the interaction between Li and resins TP 207, TP 208 and K2629. Therefore, the retention correspond to a monomolecular layer of Li^+ onto homogeneous sites within resin surfaces.

The relative position of the lines on the graph (Fig. 3) is an indication of the retention capacity of Li onto each resin. The lower the curve on the Y-axis, the more retained Li per unit mass of resin. It can be seen that the behavior of the TP 207 and TP 208 resins are very similar to each other, and slightly worse than that of the K2629 resin. This difference is accentuated at lower Ce, as was determined by analyzing the value of K_d.

3.3. Elution and reutilization studies

Samples of 50 mL of synthetic solution with $10\ mg\ L^{-1}$ Li were contacted with 1 g of resin, as described in previous sections. After contact, resin and solutions were filtered and resin was contacted with 50 mL of HCl, 3 M and 4 M. The elution of lithium was 89.8% for the

Table 5
Model parameters of ion-exchange kinetic models for Li retention onto TP 207, TP 208 and K2629 resins.

Resin	$Q_{e\text{-}exp}$ (mg/100 g)	First order			Second order			
		$Q_{e\text{-}cal}$ (mg/100 g)	k_1 (min^{-1})	R^2	$Q_{e\text{-}cal}$ (mg/100 g)	k_2 ($g\ mg^{-1}\cdot min^{-1}$)	$H = k_2Qe^2$	R^2
K2629	48.95	83.91	0.0762	0.9596	52.72	0.0600	208	0.9943
TP 207	48.95	31.70	0.1311	0.9826	53.04	0.1249	460	0.9997
TP 208	49.10	7.43	0.0892	0.7768	50.67	0.2168	844	0.9989

R^2: coefficients of determination; $Q_{e\text{-}exp}$: experimental capacity values; $Q_{e\text{-}cal}$: calculated capacity values; H: initial rate of ion-exchange; k_1 and k_2 are the first and second order kinetics constants.

Table 6
Parameters from equilibrium models.

	Langmuir model			Freundlich model			Dubinin-Radushkevic model			Temkin model		
	Q_M (mg g^{-1})	K_L (L mg^{-1})	R^2	K_F	Fr	R^2	Q_s (mg g^{-1})	K_{AD} (mol^2 kJ^{-2})	R^2	A_T (L m^{-1} g^{-1})	b_T	R^2
K2629	1.84	0.108	0.997	0.936	1.79	0.968	1.40	0.168	0.896	42.5	5714	0.862
TP 208	1.23	0.325	0.990	0.702	1.68	0.946	1.29	0.240	0.849	19.7	4628	0.882
TP 207	2.54	2.434	0.988	0.828	1.52	0.968	1.17	0.232	0.854	21.2	5692	0.919

R_L: Langmuir separation factor; Q_M: maximum monolayer coverage capacity from Langmuir model; Fr: Freundlich isotherm constant; Qs: theoretical isotherm saturation capacity; K_{AD}: Dubinin–Radushkevich isotherm constant; A_T: Temkin isotherm equilibrium binding constant; b_T: Temkin constant.

resin K2629, 80.4% for TP 207 resin and over 84.9% for TP 208 resin (Table 7). The best option to recuperate the Li retained in the resins is to employ 4 M HCl for TP 207 and K2629, but for TP 208 the elution yield is slightly higher using HCl 3 M than 4 M. Both molarities are higher than indicated by the manufacturer. After elution, resins were conditioned according to the manufacturer to H form and Na form. Once regenerated they were contacted with synthetic solutions under the same conditions as in the previous case.

After regeneration, the retention yields of K2629 are quite similar to obtained with fresh resins (Table 8). It has been proven that the K2629 resin can be regenerated to H-form or Na-form, and in both cases it still allows the recovery of Li with high capture yields (Table 8). In the case of TP 207 and TP 208, the regenerated resin behavior is similar to obtained with fresh resins when they are regenerated to Na-form, but not in H-form (Table 8). In this case, the performance of Li capture decreases drastically. This is in accordance with the recommendations of the manufacturer (R = 40.3%).

Table 7
Elution tests experimental results.

Retention yield	K2629		TP 207		TP 208	
	98.0%	98.0%	98.4%	98.4%	98.8%	98.8%
Eluting solution	HCl 3 M	HCl 4 M	HCl 3 M	HCl 4 M	HCl 3 M	HCl 4 M
Eluting yield	83.6%	89.8%	73.8%	80.4%	87.1%	84.9%

Table 8
Reutilization tests experimental results with fresh and regenerated resins.

	K2629	TP 207	TP 208
Lithium retention yield with fresh resins	98.0%	98.4%	98.8%
Lithium retention yield with regenerated Resin (in H form)	97.9%	52.2%	40.3%
Lithium retention yield with regenerated Resin (in Na form)	97.8%	98.1%	98.2%

3.4. Effect of Na content studies by response surface methodology

Tests were performed with Li and Na bearing aqueous solutions (Table 9). In the multivariable design of experiments, a set of experiments were performed with each resin and the relationship between the variables (Li and Na contents in coded terms) and responses (R and Q) was studied using regression models 10. Statistical parameters and analysis of regression parameters for the predicted response quadratic model are shown in Tables SI-3, SI-4 and SI-5. R models for the studied resins and Q for TP 208 were significant. Mathematical equations for significant models are shown in Table 10.

The average Li retention yield by the resin K2629 is 62.7%. Experimental capacities varied from 0.16 mg g^{-1} to 3.24 mg g^{-1}. Compared with the results obtained with Li-bearing solutions without Na, experimental yields and capacities decreased significantly, indicating that although Li can be recovered with K2629 resin, even in presence of Na, larger scale operation will be difficult, since the capacity of the resin is very low in the presence of large amounts of sodium.

The stat-Ease Design expert was used for ANOVA analysis of the R (for K2629 resin) model (Fig. 4). The statistical significance of the model was checked by an F-test. The model-F value of 6.31 and the probability value (Prob - F < 0.0136) implies that the model is significant (significant models has prob-F < 0.05) (Table SI-3). Adequate precision compares the range of the predicted values to the mean

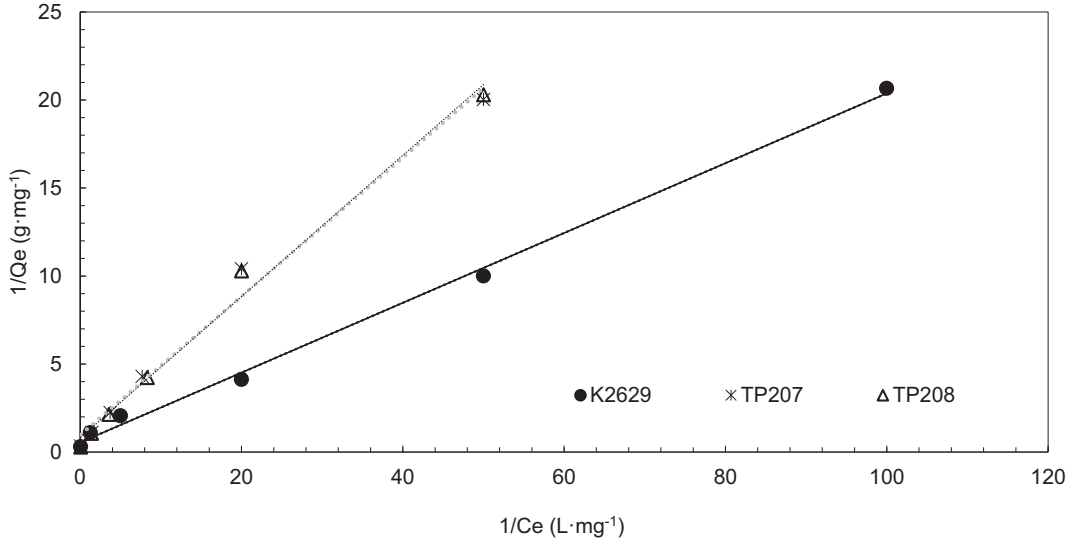

Fig. 3. Linearized Langmuir isotherms for K2629, TP 207 and TP 208 resins (Q_e capacity at equilibrium; c_e: lithium content at equilibrium).

Table 9
Experimental lithium retention yields (R) and capacity (Q) obtained for K2629, TP 208 and TP 207 in the CCRD experiments.

Run	Coded variables		K2629		TP 208		TP 207	
	Li	Na	R (%)	Q (mg g^{-1})	R (%)	Q (mg g^{-1})	R (%)	Q (mg g^{-1})
1	1	1	64.5	0.65	89.5	0.90	90.5	0.91
2	1.414	0	62.8	1.57	86.8	2.17	88.0	2.20
3	-1	1	49.2	1.23	50.4	1.26	68.0	1.70
4	0	0	64.0	1.60	87.6	2.19	88.2	2.21
5	0	0	64.8	3.24	86.7	4.34	86.0	4.30
6	0	0	61.4	2.45	80.4	3.22	80.5	3.22
7	0	0	62.2	1.56	88.0	2.2	89.0	2.23
8	0	0	66.5	2.66	89.6	3.59	89.5	3.58
9	1	-1	62.6	1.57	86.6	2.17	88.2	2.21
10	-1	-1	65.2	1.63	87.4	2.19	88.8	2.22
11	0	−1.414	67.6	1.69	89.6	2.24	90	2.25
12	0	1.414	59.0	0.59	84.0	0.84	85	0.85
13	−1.0.414	0	65.2	0.16	80.0	0.20	87.2	0.22

Table 10
Predicted models for lithium retention yields (R) and capacity (Q) for each resin (RSM).

Resin	Response	Predicted model	R^2
K2629	R (%)	62.71–3.28 Na + 1.00 Li + 4.48·Li·Na	0.678
TP 208	R (%)	83.69 + 5.59 Li – 5.25 Na + 9.98·Li·Na	0.670
	Q (mg·g^{-1})	3.13–0.52 Na +0.20 Li - 0.086 Li Na – 0.81·Li^2–0.76 Na^2	0.742
TP 207	R (%)	86.12 + 2.61 Li - 3.20 Na + 5.17 Li Na	0.630

Na: Na content in coded terms (adimensional); Li: Lithium content in coded terms (adimensional).

prediction error. The signal to noise ratio of 9.202 indicated an adequate signal. A value > 4 is desirable for a good model and indicates the predicted model could be used to navigate the design space. The correlation coefficient (R^2) shows how the model accounts for the response. A value of 0.8 is desired for the good fit of the model. In this model, R^2 is 0.678 for Lithium retention. The "Lack of fit tests" compares the residual error to pure error from replicated design points. A significant lack of fit suggests there may be some systematic variation unaccounted for the hypothesized model. In this model a "lack of fit" not significant was determined by ANOVA analysis. Based on the results, the model was considered adequate.

Final mathematical equation is a linear model (Table SI-3), in which the most significant factor is the Na content (linear coefficient: −3.28), much more influencing than the Li content (linear coefficient: +1), confirming that the performance is very sensitive to the concentration of Na. Na content affects negatively to Li retention, probably because Na moves the equilibrium to the opposite direction to the desired for the retention. In the middle of the range of study, the Li yield is 62.71 (independent term). In the range of study, Na is an important parameter, and retention could vary from 58% when Na content is the highest, to 70%, when Na content is the lowest (Fig. 4). Regarding to the Li loading capacity of K2629, the software suggest a not significant model. For this reason, the model is not shown.

In the case of TP 208 resin (Fig. 5, Table SI-4), experimental values of Li retention are in the range: 50.4%–89.6% (mean Li retention is 83.6%). The mathematical models of the retention is significant (Table SI-4) and there is a 1.32% chance that an F-value this large could occur due to noise. This model can be used to navigate the design space. In coded model, the Na content affected adversely to retention. It is a linear model, and the influence of Li and Na is almost similar (coefficients +5.59 and −5.25), so Li affects positively and Na negatively. The performance decreased in the case of solutions containing Na, the

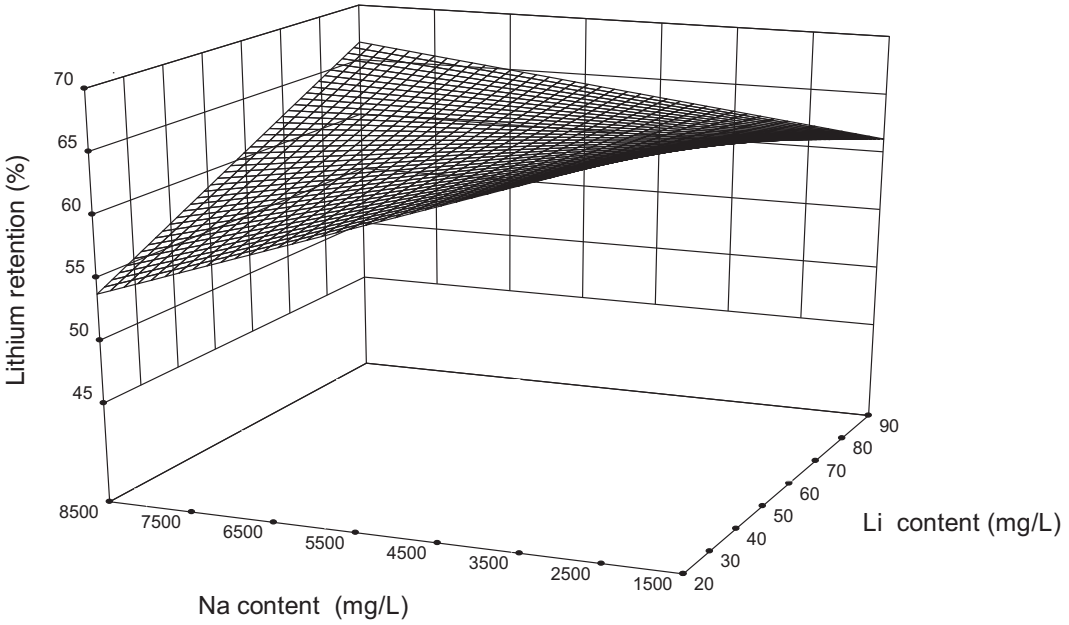

Fig. 4. RSM for lithium retention yield onto K2629 resin.

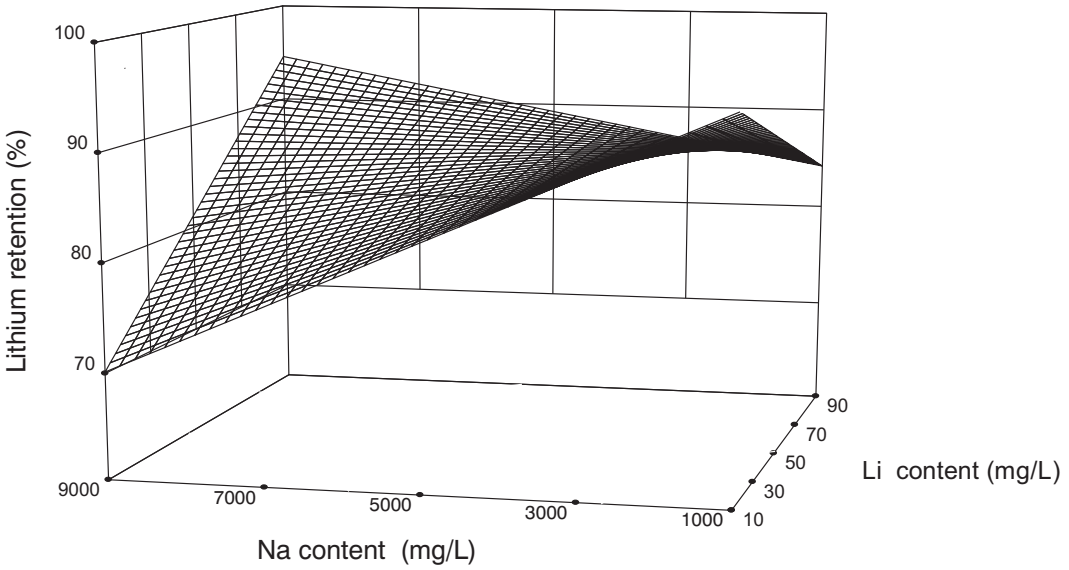

Fig. 5. Response Surface for lithium retention yield onto TP 208 resin.

higher Na, and the lesser retention yield. Comparing the results obtained in solutions without Na, both performance and capacity have lower values.

Regarding the Li loading capacity, the Model F-value of 4.02 implies there is 4.87% chance that an F-value this large could occur due to noise. So, the model is considered as significant. Model can be used to predict the TP 208 Li retention capacity. Experimental capacities varied from 0.20 to 4.34 mg g-1 (mean capacity is 0.48 mg g^{-1}).

Mean lithium retention yield onto TP 207 resin is 86.25% and the experimental capacities varied from 0.22 to 4.30 mg g^{-1}. The experimental lithium retention yields are in the range: 68.0%–90.5%. The Model F-value of 5.11 implies the model is significant and it showed an adequate signal precision (7.646), so the model can be used in the range of study. In the case of TP 207 resin, according to the mathematical model, the positive influence of lithium concentration is similar to the negative Na influence (−2.61 and −3.20, respectively), in the range studied (as it was said for TP 208).

Regarding to the Li loading capacity of TP 207 (Fig. 6, Table SI-5), the software suggest a model not significant (F-value = 3.46), and it cannot be used to navigate the design space (adequate precision = 4.525).

If results are compared with the experimental results with solutions without Na, both performance and capacity vary within the same ranges. The lithium retention yield decrease from 83% to around 68%.

According to the experimental results and to the RSM model, TP 207 and TP 208 show a better Li sorption behavior than K2629 in the presence of Na. If the performance and capacity values are compared for the same concentrations of Li with and without the presence of Na in the solution, the low yield can be seen for the three resins due to the presence of Na in solution: the decrease is more important in the case of resin K2629 than in the case of resins TP 207 and TP 208. The experimental capacities also decrease for the three resins studied due to the presence of Na in solution. This means that although the resins allow to recover Li from this type of solutions, the operation with real brines, in which the concentration of Na will be much higher than that of Li will be difficult, because the need for resin will be very high, which

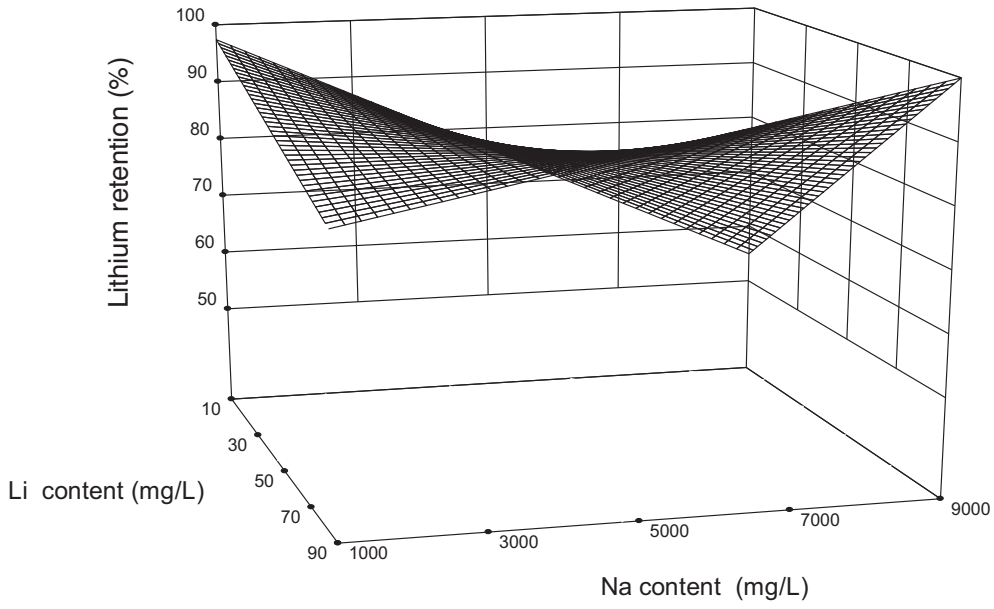

Fig. 6. Response Surface for lithium retention yield onto TP 207 resin.

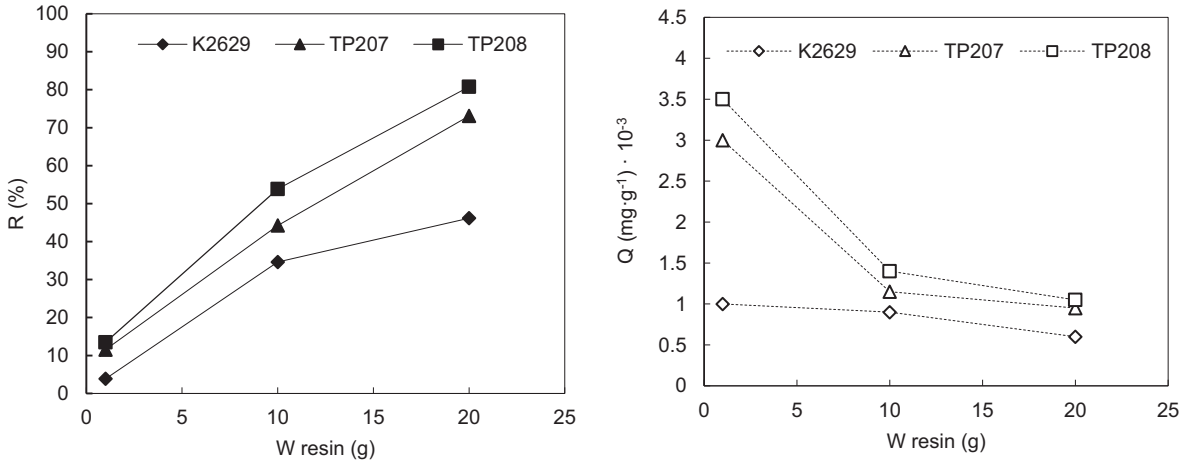

Fig. 7. Lithium retention (R, %) and capacity (Q, mg g^{-1}) for each resin with real brines.

hinder the viability of scaling this process.

3.5. Li retention from real brines

The tests were performed with samples of 50 mL of real brines and different amounts of resin (1 g, 10 g and 20 g). Li retention yield is in the range 30%–55% and 52%–80%, depending on the type of resin and the amount(Fig. 7).

In these tests TP 208 shown the maximum Li retention efficiency and loading capacity, and the lowest Li retention and loading capacity are shown for K2629. The capacities are below 10^{-3} mg g^{-1}. The capacity obtained in studies with TP 208 resin is slightly higher than with TP 207 and K2629. Both the yield and the capacity suffer a very important decrease with respect to the tests with synthetic solutions, due to the presence of other ions in the real brine (besides Li or Na). That is, there are other elements competing with the Li for the active sites of the three resins. It is necessary to add a lot of resin to keep the yield above a certain value; this causes the capacity to decrease drastically.

The Li retention yields are lower than predicted by the mathematical models developed in Section 3.4, i.e. the predicted performance is much higher than the experimental performance in the case of real brines due to the presence of high concentrations of interfering elements. Taking into account the brine composition, Mg and Ca are considered the main interfering ions. To evaluate this issue, some experiments have been carried out with a modified brine to which 99% of Ca and Mg have previously been eliminated. To do that, the necessary amount of sodium carbonate to precipitate Ca was added and pH was increased to 11.5 with NaOH, removing Ca as $CaCO_3$ and Mg as $Mg(OH)_2$. The concentration of Li after Mg and Ca precipitation is determined to be 0.52 mg·L^{-1}.

The experiments were carried out by contacting 1 g of each type of resin with 50 mL of the modified brine. Then they have been maintained in contact for 24 h to ensure equilibrium. After the contact, resin and liquid solution were separated and the Li concentration not retained by resins was measured (Table 11).

The Na and Li contents of modified brines were replaced in the mathematical models calculated in Section 3.4 (Table 11) in order to predict the Li retention yields. While the predicted retention values are higher than the experimental ones, the difference is much smaller when the Mg and Ca ions have been removed. Therefore, it can be concluded that by eliminating Ca and Mg, the Li retention is possible from the generated brines in desalination facilities; although it is necessary to take into account the partial abatement of Li due to the method of elimination of Mg and Ca.

4. Conclusions

This study shows that it is possible to recover Li from brines with ion exchange resins. For solutions in which there is only Li, the TP 207, TP 208 and K2629 resins have high retention yields (> 95%). When, in addition to Li, there is Na in solution, the retention performance is low, especially in the case of resin K2629. This tendency is much more marked in the case of using brines with other elements in solution. The resin most affected by the competitive effect of other ions in solution is K2629. The Lewatit K2629 resin is therefore very effective when used in solutions where there is no Na, or the concentration of this element is low. In other cases, it would be preferable to employ the TP207 or TP208 resins to retain Li from brines. It is also possible recovering Li from the brines generated in desalination facilities using the three studied resins if Ca and Mg are previously eliminated. in this case, the Li lost due to the method of elimination of Mg and Ca should be considered.

Regarding kinetics, the fastest retention of Li is attributed to TP208 and the slowest to K2629. The theoretical capacity sequence is found to be TP207 > K2629 > TP208, but the three values are quite similar. Results indicated that the models obtained for pseudo-second order were more suitable for the Li retention onto K2629, TP207 and TP208 resins. The better fit of the pseudo-second-order suggest that resins-Li main interaction is controlled by chemical sorption, and the retention rate depends more on the availability of the active sites than the concentration of Li in solution.

Langmuir separation factor (R_L) varied from 0 to 1 in all experiments, indicating that lithium sorption is favorable for the 3 resins. Due to the determination factors of three resins values and the

Table 11
Results obtained in experiments with modified brines.

	Modeled Li retention yield (%)	Initial Li content (mg L^{-1})	Li content at equilibrium (mg L^{-1})	Experimental Li retention yield (%)	Experimental/modeled Li retention yield
K2629	30.5	0.52	0.39	25,0	0.82
TP 207	26.1	0.52	0.40	23.1	0.88
TP 208	44.9	0.52	0.31	40.4	0.90

characteristics of resins (homogeneous sites), Langmuir model is preferred for describing the interaction between Li and resins TP207, TP208 and K2629. Therefore, the retention correspond to a monomolecular layer of Li onto homogeneous sites within resin surfaces.

Regarding desorption, yields ranged 73.8%–89.8%, achieving the highest (> 80%) when using 4 M HCl as eluting solution. It is possible to reuse regenerated resins with high yields, similar to those obtained when the resin is used for the first time.

Appendix A. Supplementary data

Supplementary data to this article can be found online at https://doi.org/10.1016/j.desal.2019.114073.

References

[1] S. Nishihama, K. Onishi, K. Yoshizuka, Selective recovery process of lithium from seawater using integrated ion exchange methods, Solvent Extr. Ion Exch. (2011), https://doi.org/10.1080/07366299.2011.573435.

[2] A. Lauren, P. Oppenheimer, World Lithium Resource Impact on Electric Vehicles, (2008).

[3] E. Siame, R.D. Pascoe, Extraction of lithium from micaceous waste from China clay production, Miner. Eng. 24 (2011) 1595–1602, https://doi.org/10.1016/j.mineng.2011.08.013.

[4] A. Yaksic, J.E. Tilton, Using the cumulative availability curve to assess the threat of mineral depletion: the case of lithium, Resour. Policy 34 (2009) 185–194, https://doi.org/10.1016/j.resourpol.2009.05.002.

[5] S. Bunani, K. Yoshizuka, S. Nishihama, N. Kabay, Application of Bipolar Membrane Electrodialysis (BMED) for Simultaneous Separation and Recovery of Boron and Lithium From Aqueous Solutions, 424 (2017), pp. 37–44, https://doi.org/10.1016/j.desal.2017.09.029.

[6] C. Jiang, Y. Wang, Q. Wang, H. Xu T. Feng, Production of lithium hydroxide from lake brines through electro–electrodialysis with bipolar membranes (EEDBM), Ind. Eng. Chem. Res. 53 (2014) 6103–6112, https://doi.org/10.1021/ie404334s.

[7] S. Kim, H. Joo, T. Moon, S.H. Kim, J. Yoon, Rapid and Selective Lithium Recovery from Desalination Brine Using an Electrochemical System, Processes & Impacts, Environmental Science, 2019.

[8] X. Liu, X. Chen, L. He, Z. Zhao, Study on extraction of lithium from salt lake brine by membrane electrolysis, Desalination 376 (2015) 35–40.

[9] X. Nie, S. Sun, X. Song, J. Yu, Further investigation into lithium recovery from salt lake brines with different feed characteristics by electrodialysis, J. Memb. Sci. 530 (2017) 185–191, https://doi.org/10.1016/j.memsci.2017.02.020.

[10] S.-Y. Sun, L.-J. Cai, X.-Y. Nie, X. Song, J.-G. Yu, Separation of magnesium and lithium from brine using a Desal nanofiltration membrane, J. Water Proc. Eng. 7 (2015) 210–217, https://doi.org/10.1016/j.jwpe.2015.06.012.

[11] B. Swain, Recovery and recycling of lithium: a review, Sep. Purif. Technol. 172 (2017) 388–403, https://doi.org/10.1016/j.seppur.2016.08.031.

[12] Chang, I.-L., Jiang, Y.-L., Shiu, J.-Y., Lin, J.-R., 2012. Process for Producing Lithium Concentrate From Brine or Seawater. US 6764584 B2. doi:https://doi.org/10.1126/science.Liquids.

[13] R. Chitrakar, H. Kanoh, Y. Miyai, K. Ooi, A new type of manganese oxide (MnO2·0.5H2O) derived from Li1.6Mn1.6O4 and its lithium ion-sieve properties, Chem. Mater. (2000), https://doi.org/10.1021/cm0000191.

[14] R. Chitrakar, H. Kanoh, Y. Miyai, K. Ooi, Recovery of lithium from seawater using manganese oxide adsorbent (H 1.6 Mn 1.6 O 4) derived from li 1.6 Mn 1.6 O 4, Ind. Eng. Chem. Res. 40 (2001) 2054–2058, https://doi.org/10.1021/ie000911h.

[15] K.-S. Chung, J.-C. Lee, W.-K. Kim, S.B. Kim, K.Y. Cho, Inorganic adsorbent containing polymeric membrane reservoir for the recovery of lithium from seawater, J. Membr. Sci. (2008), https://doi.org/10.1016/j.memsci.2008.09.041.

[16] Kim, J.-S., Chung, K.-W., Lee, J.-Y., Kim, S.-D., 2012. Method for Preparing High-purity Lithium Carbonate From Brine. 2012/0328498 A1.

[17] L.W. Ma, B.Z. Chen, X.C. Shi, K. Zhang, Li + Extraction/Adsorption Properties of Li-Sb-Mn Composite Oxides in Aqueous Medium, Trans. Nonferrous Met. Soc, China (English Ed, 2011, https://doi.org/10.1016/S1003-6326(11)60911-4.

[18] K. Ooi, Y. Miyai, S. Katoh, Recovery of lithium from seawater by manganese oxide adsorbent, Sep. Sci. Technol. 21 (1986) 755–766, https://doi.org/10.1080/01496398608056148.

[19] J. Park, H. Sato, S. Nishihama, K. Yoshizuka, Separation and recovery of lithium from geothermal water by sequential adsorption process with λ-MnO 2 and TiO2, Ion Exch. Lett. 5 (2012) 1–5, https://doi.org/10.3260/iel.2012.08.001.

[20] T. Wajima, K. Munakata, T. Uda, Adsorption behavior of lithium from seawater using manganese oxide adsorbent, Plasma Fusion Res. (2012), https://doi.org/10.1585/pfr.7.2405021.

[21] Alurralde, P., Mehta, V., 2012. Recovery of li values from sodium saturate brine. US 8309043 B2.

[22] Bauman, W.C., Burba, J.L., 2001. Composition for the recovery of lithium values from brine and process of making/using said composition. US 6280693 B1.

[23] Bauman, W.C., Burba, J.L., 1986. Intercalations of crystalline lithium aluminates. US 4727167.

[24] Bauman, W.C., Burba, J.L., 1965. Recovery of lithium from brines. US 5389349.

[25] A.H. Hamzaoui, B. Jamoussi, A. M'nif, Lithium recovery from highly concentrated solutions: response surface methodology (RSM) process parameters optimization, Hydrometallurgy 90 (2008) 1–7, https://doi.org/10.1016/j.hydromet.2007.09.005.

[26] Harrison, S., Sharma, C.V.K., Viani, B.E., Peykova, D., 2014. Lithium extraction composition and method of preparation thereof. US 8637428 B1.

[27] S. Hawash, E. Abd, E. Kader, G. El Diwani, Methodology for selective adsorption of lithium ions onto polymeric aluminium (III) hydroxide, J. Am. Sci. Am. Sci. 66 (2010) 301–309.

[28] J.M. Lee, W.C. Bauman, Recovery of lithium from brines. (1978) 4116858.

[29] J.M. Lee, W.C. Bauman, Recovery of lithium from brines. (1979) 4159311.

[30] J.M. Lee, W.C. Bauman, Recovery of lithium from brines. (1980) 4221767.

[31] J.M. Lee, W.C. Bauman, Recovery of lithium from brines. (1982) 4347327.

[32] J.M. Lee, W.C. Bauman, Lithium halide brine purification. (1983) 4376100.

[33] W.J. Repsher, K.T. Rapstein, Recovery of Lithium From Brine, (1981), p. 4291001.

[34] C.A. Borgo, A.M. Lazarin, Y.V. Kholin, R. Landers, Y. Gushikem, The ion exchange properties and equilibrium constants of Li^+, Na^+ and K^+ on zirconium phosphate highly dispersed on a cellulose acetate fibers surface, J. Braz. Chem. Soc. (2004), https://doi.org/10.1590/S0103-50532004000100010.

[35] C.A. Borgo, Y. Gushikem, Zirconium phosphate dispersed on a cellulose fiber surface: preparation, characterization, and selective adsorption of Li^+, Na^+, and K^+ from aqueous solution, J. Colloid Interface Sci. (2002), https://doi.org/10.1006/jcis.2001.8045.

[36] M. Petersková, C. Valderrama, O. Gibert, J.L. Cortina, Extraction of valuable metal ions (Cs, Rb, Li, U) from reverse osmosis concentrate using selective sorbents, Desalination 286 (2012) 316–323, https://doi.org/10.1016/j.desal.2011.11.042.

[37] H. Bukowsky, E. Uhlemann, D. Steinborn, The recovery of pure lithium chloride from "brines" containing higher contents of calcium chloride and magnesium chloride, Hydrometallurgy 27 (1991) 317–325, https://doi.org/10.1016/0304-386X(91)90056-R.

[38] Y. Khambhaty, K. Mody, S. Basha, B. Jha, Kinetics, equilibrium and thermodynamic studies on biosorption of hexavalent chromium by dead fungal biomass of marine Aspergillus niger, Chem. Eng. J. 145 (2009) 489–495, https://doi.org/10.1016/j.cej.2008.05.002.

[39] D. Wen, Y.S. Ho, X. Tang, Comparative sorption kinetic studies of ammonium onto zeolite, J. Hazard. Mater. (2006), https://doi.org/10.1016/j.jhazmat.2005.10.020.

[40] I.-H. Lee, Y.-C. Kuan, J.-M. Chern, Equilibrium and kinetics of heavy metal ion exchange, J. Chinese Inst. Chem. Eng. (2007), https://doi.org/10.1016/j.jcice.2006.11.001.

[41] K.R. Hall, L.C. Eagleton, A. Acrivos, T. Vermeulen, Pore- and solid-diffusion kinetics in fixed-bed adsorption under constant-pattern conditions, Ind. Eng. Chem. Fundam. 5 (1966) 212–223, https://doi.org/10.1021/i160018a011.

[42] T.W. Weber, R.K. Chakravorti, Pore and solid diffusion models for fixed-bed Adsorbers, AICHE J. 20 (1974) 228–238, https://doi.org/10.1002/aic.690200204.

[43] N.D. Hutson, S.C. Zajic, R.T. Yang, Influence of residual water on the adsorption of atmospheric gases in Li-X zeolite: experiment and simulation, Ind. Eng. Chem. Res. 39 (2000) 1775–1780, https://doi.org/10.1021/ie990763z.

[44] E. Voudrias, F. Fytianos, E. Bozani, Sorption description isotherms of dyes form aqueous solutions and waste waters with different sorbent materials. Glob. Nest, Int. J. 4 (2002) 75–83.

[45] S.V. Mohan, J. Karthikeyan, Removal of lignin and tannin colour from aqueous solution by adsorption onto activated charcoal, Environ. Pollut. 97 (1997) 183–187.

[46] Tabatabai, M.A., Sparks, D.L., Goldberg, S., 2005. Equations and Models Describing Adsorption Processes in Soils. doi:https://doi.org/10.2136/sssabookser8.c10.

[47] A.O. Dada, Langmuir, Freundlich, Temkin and Dubinin–Radushkevich isotherms studies of equilibrium sorption of Zn 2+ unto phosphoric acid modified Rice husk, IOSR J. Appl. Chem. 3 (2012) 38–45, https://doi.org/10.9790/5736-0313845.

[48] M. Temkin, V. Pyzhev, Kinetics of ammonia synthesis on promoted iron catalysts, Acta Physicochim. 12 (1940) 327–356.

[49] A. Dąbrowski, Adsorption - from theory to practice. Adv. Colloid Interface Sci, (2001), https://doi.org/10.1016/S0001-8686(00)00082-8.

[50] A. Günay, E. Arslankaya, I. Tosun, Lead removal from aqueous solution by natural and pretreated clinoptilolite: adsorption equilibrium and kinetics, J. Hazard. Mater. (2007), https://doi.org/10.1016/j.jhazmat.2006.12.034.

[51] M.L.H. Figueroa, B.L. Rodríguez, V.M. Miranda, Cinética e isotermas de adsorción de Pb(II) en suelo de Monterrey XI, (2008).

[52] Y.S. Ho, G. McKay, Pseudo-second order model for sorption processes, Process Biochem. (1999), https://doi.org/10.1016/S0032-9592(98)00112-5.

[53] J.M. Salman, V.O. Njoku, B.H. Hameed, Bentazon and carbofuran adsorption onto date seed activated carbon: kinetics and equilibrium, Chem. Eng. J. 173 (2011) 361–368, https://doi.org/10.1016/j.cej.2011.07.066.